

Semicontinuous silver films for protein sensing with SERS

Vladimir P. Drachev^{*a}, Mark Thoreson^a, Eldar Khaliullin^a, Andrey K. Sarychev^a, Dongmao Zhang^b, Dor Ben-Amotz^b, Vladimir M. Shalaev^a

^a School of Electrical and Computer Engineering, Purdue University, West Lafayette, IN, USA 47907

^b Department of Chemistry, Purdue University, Brown Bldg., West Lafayette, IN, USA 47907
Indiana Proteomics Consortium INPROTEO, Indianapolis, IN 46202, USA

ABSTRACT

High SERS sensitivity for protein detection has been accomplished with semicontinuous silver films. Specifically, an insulin surface density as low as 80 fmol/mm² and 25 amol in a probed area has been readily detected.

Keywords: Semicontinuous metal films, SERS of proteins, human insulin

1. INTRODUCTION

Plasmonic nanomaterials have recently attracted much interest because of their unique optical properties and novel applications that are possible with the current progress in nanofabrication. Many efforts are aimed at applying surface enhanced Raman scattering (SERS) with nanofabricated plasmonic substrates to biomolecule sensing. Among the new optical phenomena discovered in plasmonic nanomaterials are nonlinear optical activity [1], the chirality of plasmon modes [2], and the quantum-size effect in two-photon excited luminescence in silver nanostructures [3]. Large local-field enhancements for particle aggregates are of particular importance for a number of nonlinear optical phenomena [4], including the recently-observed hyper-Rayleigh scattering and two-photon excited luminescence [3]. These phenomena are closely related to the problem of surface enhanced Raman optical activity and the problem of the luminescence background that always accompanies SERS spectra. In many cases, the optical properties of a metal nanoparticle can be described in terms of electron transitions between the discrete energy states in a quantum well subjected to the enhanced local field [5]. The optical transitions between the discrete levels in metal nanostructures and their saturation results in a large background in surface-enhanced Raman scattering and the SERS spectral dependence, as well as some important features in the interaction between metal nanostructures and molecules adsorbed on their surfaces. Here we focus on the SERS of proteins deposited on a nanostructured metal surface.

SERS has proven to be a powerful mechanism for probing molecules adsorbed at a metal interface. As a result of a million-fold average enhancement it is possible to obtain high quality spectra at micromolar concentrations. SERS is also sensitive to orientation and distance from the metal surface as formulated in the so-called "surface selection rules" (see review [6] and refs. therein).

Semicontinuous metal films can be produced, for example, by vacuum evaporation or sputtering of metal onto an insulating substrate. In the growing process, small metallic grains are initially formed on the substrate. A typical size of such a metal grain can vary from 5 to 50 nm. As the film grows, the metal filling factor increases and coalescence occurs so that irregularly shaped self-similar clusters are formed on the substrate.

Metal-dielectric films exhibit anomalous optical phenomena that are absent for bulk metal and dielectric components. For example, the anomalous absorption in the near-infrared spectral range leads to unusual behavior of the transmittance and reflectance of the film. Typically, the transmittance is much higher than that for continuous films, whereas the reflectance is much lower. The local fields in a semicontinuous metal film are shown to exhibit giant fluctuations in the visible and infrared ranges when the dissipation in metallic grains is small. The field fluctuations

* vdrachev@ecn.purdue.edu

result in significantly enhanced Raman scattering from such films [7]. Metal-dielectric thin films have been used as SERS-active substrates since the 1980s [8-12]. The magnitude of the enhancement depends critically on nanostructure morphology as is shown with both theory and experiment and can be about 10^5 - 10^6 for a signal averaged over a macroscopic area.

This paper presents results of our experimental studies of SERS protein sensors based on semicontinuous silver films (SSFs). We focus on the detection limits of such sensors as well as structural and optical properties of the silver films. All of the experiments presented in this paper were performed with human insulin. We demonstrate efficient SERS detection of human insulin by using SSFs as SERS substrates. High SERS sensitivity for protein detection has been accomplished; specifically, an insulin surface density as low as 80 fmol/mm^2 (with 25 amol in the probed area) has been readily detected.

2. EXPERIMENTAL

2.1 Substrate preparation

Microscope glass slides were purchased from Fisher and were cut into 2.5 cm x 2.5 cm sections for use as initial substrates. The slides were cleaned using multiple solvent rinses, a piranha ($\text{H}_2\text{O}_2:3\text{H}_2\text{SO}_4$) acid bath, rinsing in 18 M Ω deionized water in series, and then dried with pressurized gaseous nitrogen. Silver shot was purchased from Alfa Aesar (99.9999 %, 1-3 mm) to be used as the source material for the films. The thin film deposition was performed in a modified Leybold electron-beam evaporator with an initial pressure inside the system of approximately 10^{-7} Torr. The film thickness and deposition rate were monitored with a quartz crystal oscillator. The glass slides were covered first by a sublayer of 10 nm SiO_2 followed by an Ag layer (7-8 nm) deposited at a rate of 0.05 nm/s. The substrates were used within one month after preparation.

2.2 Materials and insulin deposition

Recombinant human insulin used in this research was provided by Eli Lilly & Co. The insulin was dissolved in a 1 mM HCl water solution. The HCl was purchased from Baker. Deionized water of ultrapure grade was used. Insulin concentrations were determined from absorbance measurements at 280 nm using the extinction coefficient ϵ_{280} of $5.7 \text{ mM}^{-1} \text{ cm}^{-1}$ [13]. The solution was then diluted with HCl solution or water. Typically 2-4 μL of insulin solution was deposited on a substrate surface and then allowed to dry at a 45 degree incline substrate position. Quartz substrates were used for normal Raman spectra acquisition.

2.3 Methods

Our four-wavelength Raman system comprises an Ar/Kr ion laser (Melles Griot), a laser band-path holographic filter (to reject plasma lines) and two Super-Notch Plus filters to reject Rayleigh scattering (Kaiser Optical System), focusing and collection lenses, an Acton Research 300i monochromator with a grating of 1200 grooves/mm, and a nitrogen-cooled CCD (1340 x 400 pixels, Roper Scientific). SERS spectra were collected using an excitation wavelength of 568.2 nm laser beam with normal incidence and 45 degree scattering. An objective lens ($f/1.6$) provided a collection area of about $180 \mu\text{m}^2$. Collected light was delivered to the spectrometer via a fiber bundle. The spectral resolution was about 3 cm^{-1} . Raman spectra of insulin on quartz were collected using a He-Ne laser (632.8 nm) with a x20 objective lens and a 600 grooves/mm grating via the backscattering optical scheme. The nanostructure topography of the fabricated films was characterized by field emission scanning electron microscopy (FE SEM) and atomic force microscopy (AFM). High resolution FE SEM images were obtained through MAS Inc. (Raleigh, NC). AFM images were acquired with a Dimension 3100 (DI Veeco) using a 10 nm Si tip to obtain height profiles of the samples.

A Lambda 35 spectrophotometer (Perkin-Elmer) equipped with a Labsphere was used for spectral measurements of absorbance and reflectance. A protein distribution in the deposited spot was obtained with an Alpha-step 200 profilometer (Tencor Instruments).

3. RESULTS

3.1 Films structure and spectrophotometry

The films' nanostructure topography is well characterized by the FE SEM images at different magnifications ($\times 10\text{K}$ - $\times 200\text{K}$) along with AFM height profiles. The representative images are shown in Fig. 1a, b, c. The films appear uniform on the scale of tens of μm and higher. They consist of nanoparticles and their aggregates. The particle size is distributed in a range from 30 to 100 nm with an aspect ratio between 0.5 and 1 (a typical value is 0.8-0.9). The large-sized particles have an internal structure and more complicated shape. The RMS deviation from the average height as defined with the roughness analysis of the AFM images is about 7 nm, and the maximum height is about 30 nm. Fig. 2 shows a typical UV-VIS absorbance (lower trace) and reflectance (upper trace) spectra. Both spectra have a broad wing in the long wavelengths. Reflectance is greater than absorbance by a factor 1.4.

3.2 SERS and Raman spectra

SERS spectrum collected from the central part of an insulin spot is shown in Fig. 3a. Fig. 3b shows the same spectrum after linear polynomial background subtraction and normalization. The specific intensity, that is, the counts per second per mW (c/smW), was used for comparison purposes. The spot is deposited from a 3 μL drop of 1 μM insulin in a 0.1 mM HCl solution.

A comparison of the insulin SERS spectra with our normal Raman spectra of insulin on quartz (Fig. 3c) and with Zn-insulin in solution [14] (not shown here) suggests that strongly enhanced spectra reveal all the Raman fingerprints of insulin. Raman peaks are assigned mostly to the amide I and amide III bands of the peptide backbone vibrations, to the vibrational modes of phenylalanine (Phe) (B1, B24, B25 residues of the B chain) and tyrosine (Tyr) (A14, A19, B16, and B26)[15]. Namely, the spectra contain "indicators" of the phenylalanine-to-tyrosine ratio: two peaks at 624 (Phe) and 643 (Tyr) cm^{-1} ; the pair of tyrosine Raman markers at 832 and 850 cm^{-1} , which is the Fermi resonance doublet arising from the interaction between the ring breathing fundamental mode and the ring deformation overtone; the C-C stretching mode at 945 cm^{-1} ; phenylalanine ring modes at 1003 and 1030 cm^{-1} . The group of peaks between 1150 and 1500 cm^{-1} that can be constituted from Tyr and Phe peaks at 1176 and 1206 cm^{-1} , amide III bands at 1242 and 1267 cm^{-1} (they give the peak at 1248, Fig. 3b), -CH deformation modes at 1308 and 1342 cm^{-1} (peak at 1323 cm^{-1} in our case), a $-\text{COO}^-$ symmetrical stretching mode at 1422 cm^{-1} , and a $-\text{CH}_2$ deformation mode at 1450 cm^{-1} . The spectra also contain overlapped peaks around 1594 cm^{-1} which are usually

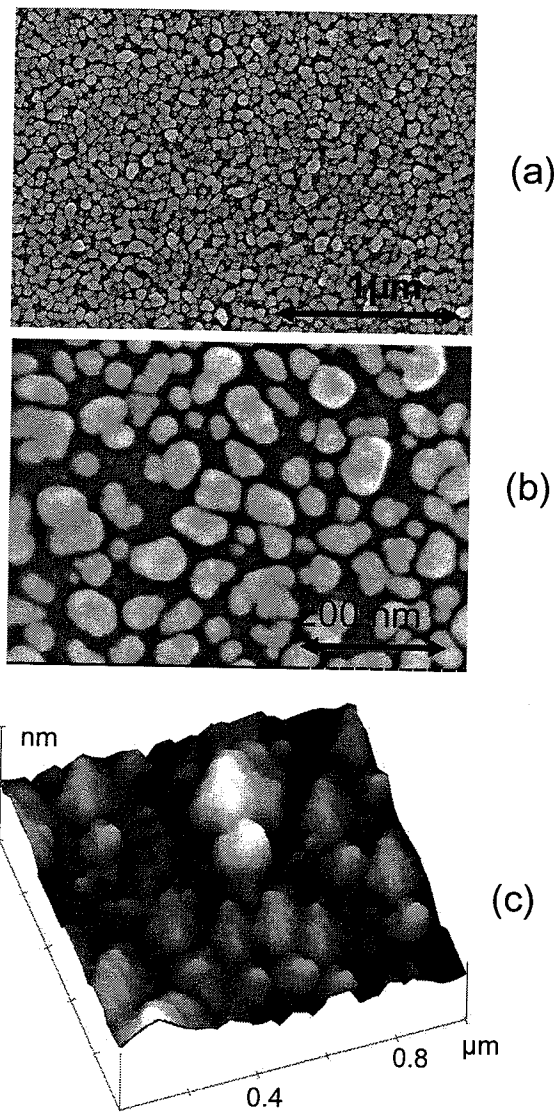


Fig. 1. Properties of Silver Semicontinuous Films. (a), (b) - FE SEM images at two different magnifications, (c) - AFM 3D image

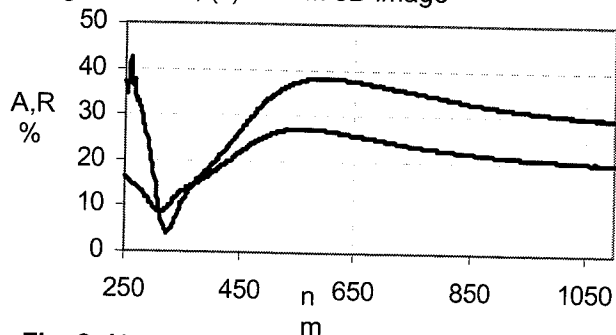


Fig. 2 Absorbance (lower, in %) and Reflectance (upper) spectra

assigned to the Phe and Tyr modes of an aromatic ring (at 1590, 1605, and 1615 cm^{-1}), and peaks around 1640 cm^{-1} and higher that are amide I modes of the α -helical (1662 cm^{-1}) and random coil (1680 cm^{-1}) structures [15]. However, there are a number of differences between the Raman and SERS spectra. There are for I_{850}/I_{832} peak intensity ratios in relative intensities of the peaks in the 1150-1500 cm^{-1} group and in the group around 1600 cm^{-1} . There is also an additional peak at 1385 cm^{-1} . Some of those differences can be attributed to alteration in the enhancement caused by orientation of the side chains relative to the metal surface; others may be due to the association of insulin molecules under liquid-solid state transition on the surface and can be seen in the Raman spectra with different hydrophobic substrates. This question will be discussed in more detail elsewhere.

3.3 Detected protein surface density and the number of proteins in the probed area.

The specific method of depositing the proteins onto the substrate surface requires special consideration for protein concentration measurement. To deposit proteins on the surface we drop 3 μL of the 1 μM insulin solution on the surface of the substrate and let it dry. As is clearly seen from the picture of the spot in Fig. 4, the spot consists of an outer ring and a central part. Our measurements with a profilometer (Fig 4) show that proteins mostly concentrate on the edges of the spot forming a ring, and the central part generally has a much lower surface concentration. Local protein surface density can be estimated as the average surface density (D_{AV}) multiplied by a distribution factor X as follows:

$$D_{loc,c} = D_{AV} X = \frac{D_{AV} \frac{S_r}{S_t} \left(\frac{h_r}{h_c} - 1\right)}{1 + \frac{S_r}{S_t} \left(\frac{h_r}{h_c} - 1\right)}$$

The distribution factor is found from the measured ratio of the ring area to the total area (S_r/S_t), and the ratio of the height at the ring to the height at the central part (h_r/h_c). Using this equation we estimate the surface density of about $80 \pm 20 \text{ fmol/mm}^2$ in the central area of the spot. A minimal molecule number in the probed area as low as 25 amol has been achieved with a laser spot of about $20 \mu\text{m}$ in diameter. The laser intensity of 450 W/cm^2 in this case is close to the upper limit for SERS spectra acquisition without incurring changes due to photomodification. The laser spot size was measured using the "knife" method.

3.4 Enhancement factor

A comparison of Raman measurements in both of the cases (our results for insulin on quartz and the results of the work [14]) gives an enhancement factor which exceeds 10^6 . To estimate the enhancement factor we first compare our SERS specific intensity with the Zn-insulin Raman in liquid. We consider the measurement systems to be very similar in both cases in terms of collection lens f-number, notch filter, resolution, and CCD capabilities. We omit the possible

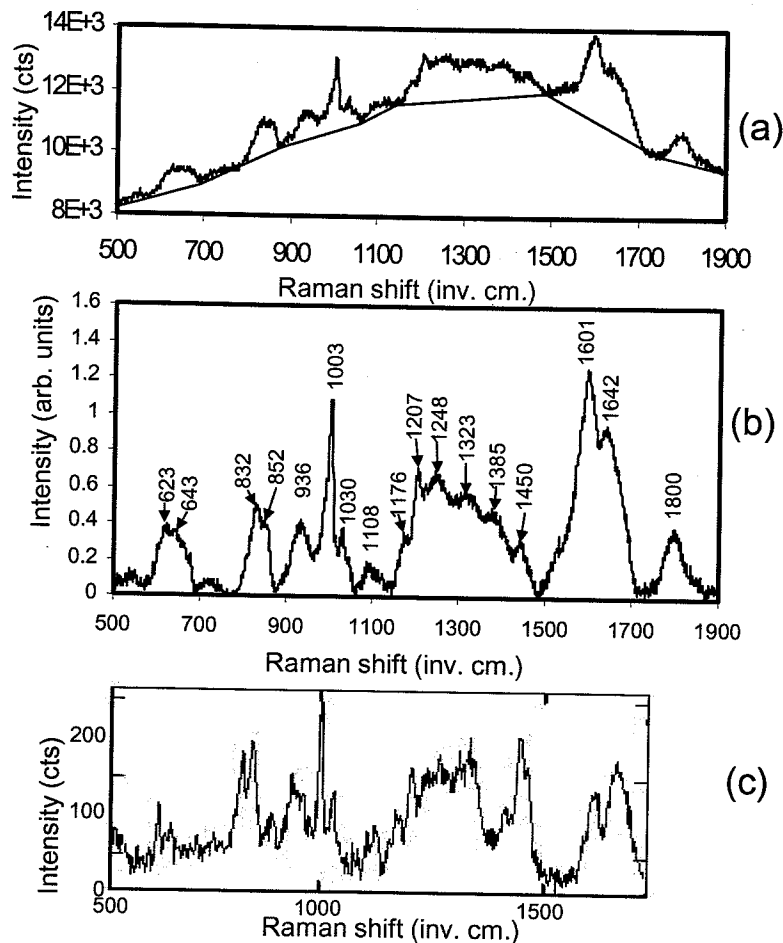


Fig. 3. Recombinant human insulin spectra, (a) – SERS spectrum of insulin on SSF, (b) – Normalized spectrum after background subtraction, normalization constant = 7cts/(s*mW), (c) – Raman spectrum of insulin on quartz substrate

differences, caused for example by additional losses in the second notch filter and the use of a fiber bundle in our case, or due to a different excitation wavelength (647.1 nm versus 568.2 nm for SERS). The intensity of the Raman signal, in general, is proportional to the intensity of the laser field and the number of molecules in the probed volume: $I_R \sim I_L N$. For the surface measurements it can be expressed through the average power W and protein surface density D as $I_L N = WD$, assuming that the collection area is equal to or exceeds the illumination area. Similar considerations give the following for volume measurements: $I_L N = WCl$, where C is concentration and l is a laser beam length in the collection volume. Finally, an estimate of the enhancement is given by $G = (J_S/J_R)(Cl/D)$, where J_S and J_R are the specific intensities (c/smW) of the 1003 cm^{-1} peak for both SERS and Raman. Under the conditions of [14], the laser beam is imaged along the monochromator slit and the length of the beam in the collection area can be estimated as approximately 7 mm [J. R. Diers, private communication]. Taking into account the other values: $J_R = 1$ c/smW, $C = 5$ nmol/ mm^3 (5 mM), $J_S = 7$ c/smW, $D_S = 80$ fmol/ mm^2 , one can get the average enhancement of about $G = 3 \times 10^6$.

To define enhancement factor under the same conditions we performed SERS and Raman measurements with the same optical system and used insulin from the same vial. Spectra were collected at 632 nm with a x20 objective lens in the backscattering configuration. The insulin spots were deposited on a quartz substrate at different insulin concentrations (10–200 μM) and volumes in the drop (5–10 μL). It was found that increasing the thickness of an insulin layer above 10 μM does not change the signal. Using this value for the penetration depth of the collection/illumination optics, one can estimate the insulin surface density D_R as 5 nmol/ mm^2 . The measured specific intensity of the Phe peak is about $J_S = 33$ c/smW for SERS and $J_R = 0.8$ c/smW for Raman. Finally, the results suggest an enhancement factor of about 2.5×10^6 . That is in a good agreement with the first estimate. We note that the local enhancement factor in the “hot spots” (where plasmons are located) is by several orders of magnitude greater than the average and can reach $\sim 10^{10}$ [4].

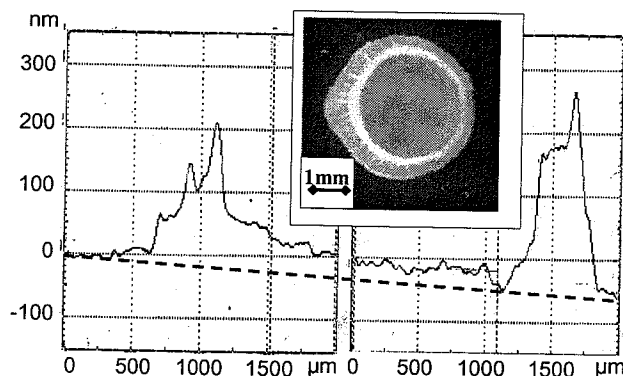


Fig. 4. Profilometry of the insulin spot on Semicontinuous Silver Film. Baseline –dashed. The areas of the ring and the spot were measured from the photograph (insert).

4. CONCLUSIONS

Nanostructured silver films demonstrate high SERS sensitivity for protein detection. The detected insulin surface density of about 80 fmol/ mm^2 means that one molecule is placed in the area of 4.6 nm x 4.6 nm. The measured average enhancement factor of the SERS-active silver structure exceeds 10^6 . Note that all typical insulin vibrational modes are enhanced approximately by the same factor.

ACKNOWLEDGEMENTS

We thank L. Rokhinson for his assistance with AFM imaging. This work was supported by INPROTEO grant.

REFERENCES

- [1] V.P. Drachev, S.V. Perminov, S.G. Rautian, and V.P. Safonov, "Giant Nonlinear Optical Activity in Aggregated Silver Nanocomposites", *JETP Letters*, **68**, 651-656 (1998).
- [2] V. P. Drachev, W. D. Bragg, V. A. Podolskiy, V. P. Safonov, W. Kim, Z. C. Ying, R. L. Armstrong, and V. M. Shalaev, "Large Local Optical Activity in Fractal Aggregates of Nanoparticles", *J. of Opt.Soc.Am. B*, **18**, No. 12, 1896-1903 (2001).
- [3] V. P. Drachev, W. Kim, V. P. Safonov, V. A. Podolskiy, N. S. Zakovryazhin, V. M. Shalaev, and R. A. Armstrong, "Low-threshold Lasing and Broad-band Multiphoton-excited Light Emission from Ag Aggregate-adsorbate Complexes in Microcavity", *J. of Modern Optics*, **49**, No. 3/4, 645-662 (2002).
- [4] V. M. Shalaev, "Nonlinear Optics of Random Media: Fractal Composites and Metal-Dielectric Films", *STMP* 158, Heidelberg (Springer 2000).
- [5] S. G. Rautian, "Nonlinear Saturation Spectroscopy of the Degenerate Electron Gas in Spherical Metallic Particles", *Sov. Phys. JETP*, **85**, 451-461 (1997).

- se,
al,
~
as
ve
he
ne
er
- [6] M. Moskovits, "Surface-enhanced Spectroscopy", *Rev. Mod. Phys.*, **57**, 783-826 (1985).
[7] P. Gadenne, D. Gagnot, M. Masson, "Surface Enhanced Resonant Raman Scattering Induced by Silver Thin Films Close to the Percolation Threshold", *Physica A* **241**, 161 (1997); P. Gadenne, F. Brouers, V.M. Shalaev, A. K. Sarychev, "Giant Stokes Fields on Semicontinuous Metal Films", *J. Opt. Soc. Am. B* **15**, 68 (1998)
[8] F. Brouers, S. Blacher, A. N. Lagarkov, A. K. Sarychev, P. Gadenne, V. M. Shalaev, "Theory of Giant Raman Scattering from Semicontinuous Metal Films", *Phys. Rev. B* **55**, 13234 (1997)
[9] M. Moskovits, "The Dependence of the Metal-molecule Vibrational Frequency on the Mass of the Adsorbate and its Relevance to the Role of Adatoms in Surface-enhanced Raman-scattering", *Chem. Phys. Lett.* **98**, 498 (1983)
[10] I. Pockrand and A. Otto, "Coverage Dependence of Raman-scattering From Pirydine Adsorbed to Silver-vacuum Interfaces", *Solid State Commun.* **35**, 861 (1980)
[11] G. Ritchie and C. Y. Chen, in "Surface Enhanced Raman Scattering", edited by P. K. Chang and T. E. Furtak, p. 361, Plenum Press, New York (1982)
[12] J. P. Davies, S. J. Pachuta, R. G. Cooks and M. J. Weaver, "Surface-enhanced Raman-scattering from Sputter-deposited Silver Surface", *Anal. Chem.* **58**, 1290 (1986)
[13] R. R. Porter, "Partition Chromotography of Insulin and Other Proteins", *Biochem. J.* **53**, 320-328 (1953).
[14] D. Ferrari, J. R. Diers, D. F. Bocian, N. C. Kaarsholm, and M. F. Dunn, "Raman Signature of Ligand Binding and Allosteric Conformation Change in Hexameric Insulin", *Biopolymers (Biospectroscopy)*, **62**, 249-260 (2001).
[15] N.-T. Yu and C. S. Lu, "Laser Raman Spectra of Native and Denatured Insulin in the Solid State", *J. Am. Chem. Soc.*, **94**, 3250 (1972).